Biotechnology Reports 43 (2024) e00851

Contents lists available at ScienceDirect

Biotechnology Reports

journal homepage: www.elsevier.com/locate/btre

Research Article

A fusion protein designed for soluble expression, rapid purification, and enhanced stability of parasporin-2 with potential therapeutic applications

Monrudee Srisaisap [a], Thanya Suwankhajit [b], Panadda Boonserm [a,*]

[a] Institute of Molecular Biosciences, Mahidol University, Phuttamonthon Salaya, Nakhon Pathom 73170, Thailand
[b] Undergraduate Program in Biological Sciences, Mahidol University International College, Mahidol University, Phuttamonthon Salaya, Nakhon Pathom 73170, Thailand

ARTICLE INFO

Keywords:
Parasporin-2
Bacillus thuringiensis
Maltose-binding protein
Cytotoxicity
Anti-cancer

ABSTRACT

Bacillus thuringiensis parasporin-2 (PS2Aa1 or Mpp46Aa1) selectively destroys human cancer cells, making it a promising anticancer agent. PS2Aa1 protoxin expression in *Escherichia coli* typically results in inclusion bodies that must be solubilized and digested by proteinase K to become active. Here, maltose-binding protein (MBP) was fused to the N-terminus of PS2Aa1, either full-length (MBP-fPS2) or truncated (MBP-tPS2), to increase soluble protein expression in *E. coli* and avoid solubilization and proteolytic activation. Soluble MBP-fPS2 and MBD-tPS2 proteins were produced in *E. coli* and purified with endotoxin levels below 1 EU/μg. MBP-fPS2 was cytotoxic against T cell leukemia MOLT-4 and Jurkat cell lines after proteinase-K digestion. However, MBP-tPS2 was cytotoxic immediately without MBP tag removal or activation. MBP-tPS2's thermal stability also makes it appropriate for bioproduction and therapeutic applications.

1. Introduction

Bacillus thuringiensis is a gram-positive endospore-forming bacterium that produces parasporal proteins during vegetative and sporulating stages. The most well-known Bt parasporal proteins are δ-endotoxin protein crystals or insecticidal crystalline proteins (ICPs) [1]. Owing to their specific insecticidal activities against lepidopteran, dipteran, and coleopteran insect pests, crystal proteins are the most explored Bt-derived proteins as a biopesticide as well as for the biological control of insects of medical importance, such as dengue, zika virus, chikungunya, yellow fever, malaria, and filariasis [2]. Once ingested by insect larvae, these protein crystals are solubilized in the midgut and are then proteolytically activated by midgut proteases. The activated proteins bind specific receptors in the insect cell membrane, leading to cell disruption and insect death [3]. However, non-insecticidal Bt strains have been widely discovered to produce human cancer cell-killing proteins, which have been named parasporins [4,5]. So far, six families of parasporins, formerly known as PS1-PS6 or Mpp and Cry classes for a new nomenclature [6], have been identified, each exhibiting a specific spectrum and mechanism of action against human cancer cells [7]. Based on their structures, parasporins can be classified into the three-domain type and the β-pore-forming-toxin (β-PFT) type [8].

Parasporin-2Aa1 (PS2Aa1, also classified as Cry46Aa1 or Mpp46Aa1 as a new name) is a member of the parasporin family with the β-pore-forming-type structure that has been intensively studied for its cytotoxic effects on a variety of human cancer cells [6,9,10]. Like Bt crystal proteins, PS2Aa1 is synthesized as intracellular parasporal crystals that require solubilization and proteolytic processing to become active [7]. The processing of PS2Aa1 from a 37-kDa precursor protein by proteinase K digestion, both at the N- and the C-termini, results in an active 30-kDa toxin [10]. It was found that the N-terminal processing of PS2Aa1 by cleaving the first 51 amino acids was essential for the cytotoxicity, whereas the C-terminal processing was not essential but did enhance the activity [10]. In its active form, PS2Aa1 is toxic to HepG2, Caco-2, MOLT-4, Jurkat, and HL-60 cell lines but does not exert any toxicity to normal cells [10–12]. It has been demonstrated that a glycosylphosphatidylinositol (GPI)-anchored protein is required for the effective cytocidal action of PS2Aa1 [13,14]. It has also been suggested that N-aminopeptidase (APN) could be a receptor in the PS2Aa1 mode of action [15,16]. Following receptor binding, pore formation leads to modifications of the cytoskeletal structures, organelle fragmentation, changes in cell morphology such as cell enlargement, and finally, cell death [10]. The mode of cell death induced by PS2Aa1, however, appears to be controversial as both non-apoptotic and apoptotic-induced

* Corresponding author.
E-mail address: panadda.boo@mahidol.ac.th (P. Boonserm).

https://doi.org/10.1016/j.btre.2024.e00851
Received 26 April 2024; Received in revised form 2 August 2024; Accepted 4 August 2024
Available online 5 August 2024

cell death have been reported [10,12,13,17,18]. Because PS2Aa1 can distinguish and destroy certain types of cancer cells without harming normal cells, its application as an alternative anticancer agent has been regarded as highly promising [12].

It has been challenging to express recombinant PS2Aa1 in *Escherichia coli* due to the protein's formation of intracellular inclusion bodies. To obtain an active form of the PS2Aa1, solubilization of inclusion bodies under a strong alkaline condition and proteinase K activation are required [10,16,19]. In the production of recombinant proteins, the ability of certain highly soluble proteins to enhance the solubility of their fusion partners is often exploited [20]. This includes the maltose-binding protein (MBP), which has been used extensively to prevent the formation of inclusion bodies, particularly in *E. coli*, where the limited solubility of recombinant proteins is a problem [21–23]. MBP appears to have chaperone-like activity by promoting the solubility, folding, and stability of its fusion protein [24,25].

In this study, we utilized maltose-binding protein (MBP) as a chaperone fused to the recombinant PS2Aa1, both full-length (fPS2) and N-terminal truncated (tPS2) forms, to eliminate the need for solubilization, and proteolytic activation processes. MBP-fPS2 and MBP-tPS2 were successfully expressed in a soluble form, and their cytotoxicity against human leukemic cancer cell lines relative to normal cells was evaluated. MBP-fPS2 exerted specific cytotoxicity against human leukemic Jurkat and MOLT-4 cells only after being digested by proteinase-K, whereas MBP-tPS2 exerted cytotoxicity directly without removing the MBP tag and proteinase K activation. MBP-tPS2 was also shown to be active after 24 h of incubation at 37 °C. To the best of our knowledge, this is the first report to provide an effective strategy for producing cytocidal PS2Aa1 as an MBP-fusion protein to enhance the solubility and stability of the protein for future investigations toward its biological function and potential therapeutic applications.

2. Materials and methods

2.1. Construction of expression vectors

The full-length *PS2Aa1* (*fPS2*) and N-terminal truncated *PS2Aa1* (*tPS2*) genes lacking the first 51 amino acids were de novo synthesized (GenScript Company, USA) based on the available protein sequence of PS2Aa1 (NCBI accession number AB099515.1) with codon optimization for prokaryotic expression and cloned into *Nde*I-5′ and *Bam*HI-3′ recognition sites of pMAL-c4x expression vector (New England Biolabs, UK) to fuse with maltose-binding protein (MBP) at the N-terminus of PS2Aa1-coding gene. After confirming the identity of the constructs by DNA sequencing, recombinant plasmids were introduced into *E. coli* BL21 (DE3)pLysS strain for protein production.

2.2. Expression and purification of the recombinant PS2 fusion proteins

E. coli BL21(DE3)pLysS cells transformed with the recombinant plasmid harboring MBP-fPS2 or MBP-tPS2 were grown in LB medium supplemented with 100 μg/mL of ampicillin and 34 μg/mL of chloramphenicol. Expression of MBP-fPS2 or MBP-tPS2 fusion protein was induced by adding 0.2 mM IPTG to an exponential growth culture and further incubated for 5 h at either 37 °C or 18 °C with shaking at 220 rpm. Cultured cells were harvested by centrifugation at 6000 rpm for 10 min at 4 °C. The harvested cells containing MBP-fPS2 or MBP-tPS2 were resuspended in an ice-cold Tris buffer (50 mM Tris–HCl pH 8.0, 200 mM NaCl, and 1 mM DTT) and completely lysed by ultrasonication. The soluble and insoluble forms of the extracted protein were separated by centrifugation at 9500 rpm for 1 h at 4 °C. The supernatant was filtered using 0.45 μm PES Filter Media before being loaded into the 5 mL MBPTrap HP column (Cytiva) equilibrated with Tris buffer. Non-specific bound proteins were removed by washing with a Tris buffer, and MBP-fPS2 or MBP-tPS2 was eluted with a Tris buffer containing 10 mM maltose monohydrate.

The MBP-fPS2 was later digested with 1 uL of 1 mg/mL Factor Xa at 25 °C overnight, followed by being activated by proteinase K using proteinase K-to-toxin mass ratio of 1:100 at 37 °C for 45 min, while the MBP-tPS2 was cut by only Factor Xa overnight to separate MBP from the recombinant PS2Aa1. Subsequently, the reactions were stopped by phenylmethylsulfonyl fluoride (PMSF) addition. The protein samples were dialyzed in 1 × phosphate-buffered saline PBS, pH 7.4 overnight at 4 °C using a 12,000–14,000-Da cut-off dialysis membrane. The samples were applied to the MBPTrap HP column (Cytiva) equilibrated with PBS, pH 7.4 to separate the cleaved MBP and recombinant PS2Aa1 proteins. The proteinase K-activated MBP-fPS2 was further purified to remove proteinase K by size-exclusion chromatography (Superdex 200 h 10/30 column, GE Healthcare Life Science). Protein quality and quantity were estimated by SDS-PAGE and a Bradford assay, respectively.

The recombinant His-tagged PS2Aa1 (His_6-fPS2) was expressed as an insoluble protoxin of 37 kDa as described previously [19]. Briefly, the inclusion bodies containing His_6-fPS2 were dissolved in 50 mM Na_2CO_3 buffer (pH 10.5) at 37 °C for 1 h. The soluble PS2 was purified by HisTrap Ni^{2+} column chromatography and was activated by proteinase K using a proteinase K-to-toxin mass ratio of 1:100 and incubated at 37 °C for 30 min to generate activated PS2Aa1. The activated proteins were further purified by gel filtration with 1 × phosphate-buffered saline (PBS, pH 7.4), analyzed by 12 % SDS–PAGE and their concentration was determined by the Bradford method using bovine serum albumin as the standard. Purified toxins were filtered with endotoxin-free sterile membrane filters (0.22 μm pore size) and stored at −20 °C until further use.

2.3. Preparation of polyclonal antibody against PS2Aa1

New Zealand white rabbits were purchased from the National Laboratory Animal Center, Mahidol University, Thailand. The animal study protocol was approved by the Institute of Molecular Biosciences Animal Care and Use Committee (IMB-ACUC) (COA. NO. IMB-ACUC 2022/001). Immunization was performed following the protocol as described previously [26]. A rabbit was primed by subcutaneous injection in the back region with 250 μg of the purified proteinase K-activated PS2Aa1 (from a recombinant His_6-fPS2) in 500 μl of PBS solution emulsified in an equal volume of TiterMax Gold adjuvant (Sigma-Aldrich, Inc., Saint Louis, MO, USA). Two weeks later, the rabbit was given a booster injection with 250 μg of PS2Aa1 antigen in PBS without adjuvant via the subcutaneous route. On days 14 and 28, after boosting, the immunized rabbit was bled, and antiserum was tested for antibody titer against the PS2Aa1 by indirect ELISA.

2.4. Western blot analysis

The recombinant protein expression was analyzed by 12 % SDS-PAGE and western blot analysis. The proteins were separated on polyacrylamide gels (12 %) and transferred on nitrocellulose membranes (GE Healthcare Life Science). Membranes were blocked with PBS containing 0.1 % Tween-20 and 5 % skimmed milk for 1 h at room temperature, probed with PS2Aa1 polyclonal antibody at a 1:2000 ratio and incubated overnight at 4 °C. Membranes were then washed in PBS containing 0.1 % Tween-20 and incubated with 1:5000 anti-rabbit IgG HRP secondary antibody (Sigma-Aldrich, Inc., Saint Louis, MO, USA) for 1 h at room temperature. After washing the membrane three times with PBS, the detection was performed using enhanced chemiluminescence reagent (ECL) as described by the manufacturer (GE Healthcare Life Science). The protein bands were finally observed using AZURE C400.

2.5. Cell lines culture and cytotoxicity analyses

Human foreskin fibroblast cell line Hs68 (ATCC CRL-1635), T-acute lymphoblastic leukemia cells lines: MOLT-4 (ATCC CRL-1582) and Jurkat (ATCC TIB-152T) were purchased from American Type Culture

Collection (ATCC, Manassas, VA, USA). Hs68 cells were cultivated in Dulbecco's modified eagle medium (DMEM) (Gibco) supplemented with 10 % fetal bovine serum (FBS) (Gibco) and 1 % penicillin and streptomycin (Gibco) and maintained at 37 °C in a 5 % CO_2 incubator. MOLT-4 and Jurkat cells were cultivated in RPMI-1640 medium (ATCC 30–2001) supplemented with 10 % of fetal bovine serum (FBS) and 1 % penicillin and streptomycin and maintained at 37 °C in a 5 % CO_2 incubator.

Briefly, Hs68, MOLT-4, and Jurkat cells were grown at about 2×10^4 cells/well in 96 well plates under sterile conditions until approximately 80 % confluence was reached. Cells were then treated with different concentrations of MBP-fPS2, MBP-tPS2, or His_6-fPS2 protein samples in a range of 0.004- 0.5 μg/mL, whereas PBS (pH 7.4) buffer was used as a mock control (MC). Cell morphologies were also observed after toxin treatments under an inverted light microscope (Nikon Eclipse TS100) with a 10 × objective lens at 24 h post-inoculation. The level of cytotoxicity was evaluated by 3-(4,5-dimethylthiazol-2-yl)−2,5-diphenyltetrazolium bromide (MTT) assay. Briefly, the MTT solution (Invitrogen) was added to the treated cells at a final concentration of 0.5 mg/mL and incubated at 37 °C for 4 h in dark to generate formazan crystals. Finally, 100 μL dimethyl sulfoxide (DMSO) (Merck) was added to dissolve the crystals and the absorbance was measured after 10 min at 595 nm using Multimode detector DTX 880 ELISA plate reader (Beckman Coulter). The percentage of cell viability was determined by comparing the absorbance of each sample with that of the negative control, and the IC_{50} value was calculated as the test sample concentration required for 50 % cell growth inhibition using GraphPad Prism 10.0 (Prism; GraphPad Software, Inc).

2.6. Endotoxin assay

To remove endotoxin, the protein solutions were treated with 1 % Triton X-114 on ice. After warming the reaction to 37 °C, the detergent phase containing the endotoxins was precipitated by centrifugation at 3000 g for 15 min, and the protein was recovered in the aqueous phase. To determine the endotoxin level in purified recombinant PS2Aa1 protein samples, the ToxinSensor Chromogenic LAL Endotoxin Assay Kit (GenScript Company, USA) was performed following the manufacturing instructions. Firstly, 100 μL of protein samples, standards, and endotoxin-free water were added to endotoxin-free vials. Then, 100 μL of LAL reagent was added, mixed, and incubated at 37 °C for 50 min. After adding 100 uL of the chromogenic substrate solution, the samples were incubated at 37 °C for 6 min. Then, 500 μL of color-stabilizers #1, #2, and #3 were added, respectively. Lastly, 200 μL of each solution was transferred from vials to a 96 well-plate. The measurement was set at 545 nm wavelength by using an EZ read 2000 microplate reader.

2.7. Functional stability assay

To determine the functional stability of purified His_6-fPS2 and MBP-tPS2, the proteins were incubated at 37 °C for different time points. The precipitated and soluble fractions were separated by centrifugation at 12,000 g for ten minutes after incubation at each time point. Using the MTT assay, the antiproliferative activity of the soluble protein after 37 °C incubation at each time point was compared to that of the unincubated protein. The protein samples were fractioned by SDS-PAGE and subjected to western blot analysis, as described above.

2.8. Statistical analysis

All experiments were performed using at least three independent replicates. All data are represented as mean ± SD, and the statistical tests were conducted using GraphPad Prism 10.0 (Prism; GraphPad Software, Inc). Two-way ANOVA was used for comparisons between several groups and a control group. Significance levels are denoted as follows: ns (no significance) $p > 0.9$, * $p < 0.1$, ** $p < 0.01$, *** $p < 0.001$, and **** $p < 0.0001$.

3. Results and discussion

3.1. Enhanced solubility of recombinant parasporin-2 via MBP fusion

Parasporin proteins are produced as crystal proteins in Bt strains. These proteins are subsequently solubilized under alkaline conditions. Following solubilization, the proteins are activated by appropriate proteases to exert cytotoxicity against cancer cells [7]. *E. coli* serves as a convenient platform for protein expression and purification. Nevertheless, the expression of the PS2Aa1 protein in *E. coli* led to the formation of inclusion bodies, impeding the purification process. In our previous study, it was found that the PS2Aa1 protein, which was tagged at its N-terminus with a hexa-histidine sequence, was expressed in *E. coli* BL21 (DH3)pLysS cells as a 37-kDa protein accumulated in inclusion bodies. Reducing the induction temperature to 18 °C, however, did not enhance protein solubility [19]. Various fusion tag proteins are available to improve the solubility of recombinant fusion partners, including the well-known MBP, NusA, thioredoxin (TrxA), GST, SUMO, and other novel elements [27]. MBP has been shown to be more successful than other fusion tag proteins in terms of target protein production and folding [23,28,29]. Therefore, in this study, we utilized MBP as a chaperone fused to the full-length PS2Aa1 at its N-terminus, hereafter referred to as MBP-fPS2, to enhance the protein solubility, thereby eliminating the need for solubilization.

Another constraint associated with the therapeutic utilization of PS2Aa1 involves the necessity for proteolytic activation. It has been demonstrated that the PS2Aa1 is cleaved by proteinase K not only at the N terminus but also at the C terminus, resulting in the generation of 31- and 30-kDa core fragments, respectively [10]. The 31-kDa corresponded to the N-terminal processing of the first 51 amino acids, whereas the 30-kDa fragment resulted from further processing at the C-terminus by cleaving off 32 amino acids, corresponding to amino acid residues 52–306. The cytotoxicity of these two processed fragments was found to vary among different cancer cell types. Both 31- and 30-kDa proteinase K-activated PS2Aa1 fragments exhibited comparable cytotoxicity against MOLT-4, Jurkat, HL-60, and HepG2 cells; however, the 30-kDa fragment caused significantly more rapid cell injury [10]. These results indicate that the N-terminal processing of PS2Aa1 was essential for its cytotoxicity, whereas the C-terminal processing was not essential but did enhance the activity. This study also constructed the N-terminally truncated PS2Aa1 lacking the first 51 amino acids by fusing with the MBP tag (MBP-tPS2) to bypass the solubilization and proteolytic activation steps (Fig. 1).

Expression of both MBP-fPS2 and MBP-tPS2 recombinant proteins was mediated by the T7 promoter of the pMAL-c4X expression vector and was induced by 0.2 mM IPTG addition under two different temperature conditions at 37 °C and 18 °C. The expression and solubility levels of the proteins in the total cell extracts, soluble fractions, and insoluble fractions were then analyzed using SDS-PAGE and quantified by gel electrophoresis image analysis software (GelAnalyzer). At 37 °C, most fusion proteins appeared to form inclusion bodies in the cell pellet fractions with molecular masses of approximately 80 kDa and 70 kDa, corresponding to MBP-fPS2 and MBP-tPS2 fusion proteins, respectively (Fig. 2A, 2B). Less than ~60 % of the MBP-PS2 fused proteins were expressed in a soluble form (Fig. 2C). Lowering the temperature to 18 °C after IPTG induction markedly enhanced the solubility of MBP-fPS2 and MBP-tPS2 proteins, corresponding to more than ~70 % in the supernatant fraction (Fig. 2C). Approximately 0.7 mg/mL of soluble fusion proteins were produced per liter of the induced cultures of the MBP-fPS2 and MBP-tPS2. Based on these results, the induction temperature of MBP-fPS2 and MBP-tPS2 was set to 18 °C for subsequent experiments.

Purification of MBP-PS2 fused proteins was conducted using amylose affinity chromatography (Fig. 3A, 3C). The supernatant containing soluble MBP-fPS2 or MBP-tPS2 obtained from *E. coli* lysate was applied to the amylose resin column equilibrated with the column buffer (see Methods). MBP-fused PS2 proteins were then eluted from the column in

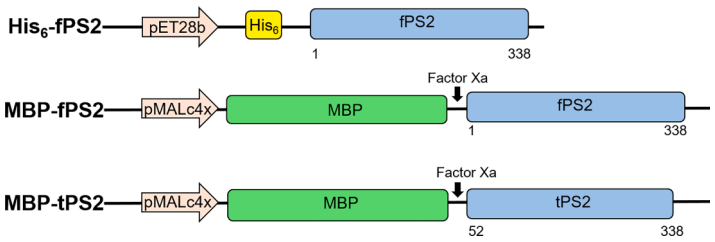

Fig. 1. Schematic representation of His_6-fPS2, MBP-fPS2, and MBP-tPS2 fusion proteins. The expression vectors used for construction, locations of fusion tags (MBP and His_6), and cleavage sites of Factor Xa are demonstrated. The amino acid residues are numbered according to the PS2Aa1 sequence.

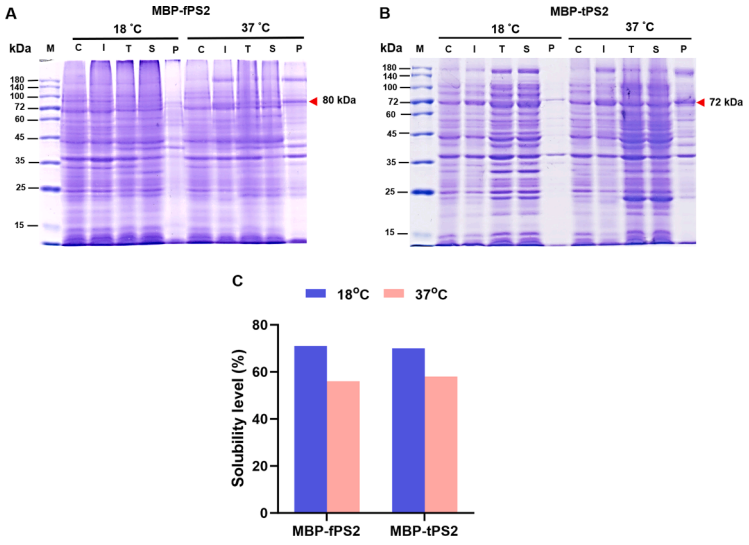

Fig. 2. Expression of the MBP-fPS2 and MBP-tPS2 fusion proteins in *E. coli* BL21(DE3)pLysS host cells. Expression of MBP-fPS2 (A) and MBP-tPS2 (B) was induced with 0.2 mM IPTG at 18 °C or 37 °C. M, molecular weight markers; C, total cell proteins before IPTG induction as a negative control; I, total cell proteins after IPTG induction; T, total proteins after sonication; S, soluble fraction after cell sonication; P, pellet fraction after cell sonication. (C) Protein solubility (%) at 18 °C or 37 °C was estimated based on the density ratio of soluble fusion protein to total fusion protein. The arrow indicates the molecular masses of the expected fusion proteins.

the same buffer containing 10 mM maltose and appeared in the elution fractions of sufficient homogeneity (Fig. 3B, 3D). Western blot analysis using the polyclonal PS2Aa1 antibody confirmed the identity of PS2Aa1 proteins expressed in both full-length and truncated forms (Fig. 4B).

To remove the MBP tag from the MBP-PS2 fusion proteins, Factor Xa was added to the purified MBP-fPS2 and MBP-tPS2, where its recognition site is located between MBP and recombinant PS2Aa1. When Factor Xa was applied overnight at 25 °C, the majority of MBP-PS2 fusion proteins were cleaved, giving expected fragments of 42 kDa for MBP and 37 kDa for the full-length and 31 kDa for the N-terminally truncated PS2Aa1 (Fig. 3B, 3D). The cleaved proteins were then dialyzed and applied to an amylose-resin column to separate the cleaved MBP tag from the PS2Aa1 protein. However, the Factor Xa-cleaved MBP-fPS2 and MBP-tPS2 were present in the flow-through fractions, which still appeared as two fragments of MBP and PS2Aa1 (either full-length or truncated form) observed by SDS-PAGE (data not shown), suggesting that MBP and PS2Aa1 still formed a complex that could not be separated by amylose affinity chromatography. An attempt was made to separate the cleaved MBP tag from the PS2Aa1 proteins by using an anion exchange chromatography; however, less than half of the cleaved MBP could be removed from the MBP-PS2 complex (data not shown), indicating that MBP remained bound to the PS2Aa1 protein following Factor Xa cleavage.

To generate an activated form of PS2Aa1, the MBP-fPS2 was incubated with proteinase K at 37 °C for 45 min, followed by SDS-PAGE and western blot analyses. Following proteinase-K digestion, the proteinase-activated PS2Aa1 revealed a protein fragment with a molecular mass of around 31 kDa, as well as a smaller fragment of around 30 kDa (Fig. 4A), which were eluted from the gel-filtration chromatography at separate peaks. The size of the latter fragment was shown to be dependent on the duration of proteinase K activation. We found that both individual proteinase K-activated fragments were also generated from the His_6-fPS2 (Fig. 4A). According to the previous study, 31- and 30-kDa proteinase K-activated fragments exhibited comparable cytotoxic effects against MOLT-4, Jurkat, HL-60, and HepG2 cells [10]. Additionally, we found that the MBP was resistant to proteinase K digestion when fused with the recombinant PS2Aa1. In contrast, the MBP alone was susceptible to proteolysis by proteinase K after 45 min of incubation at 37 °C, as shown by the disappearance of the 42-kDa band on SDS-gel (Supplementary Figure S1). This observation suggests that the association between MBP and PS2Aa1 confers benefits for the proper folding of both PS2Aa1 and MBP molecules into core fragments that are resistant to non-specific protease degradation.

The proteinase K-activated MBP-fPS2 was then subject to gel-filtration chromatography to separate the proteinase K; however, the MBP was still co-eluted with the proteinase K-cleaved PS2Aa1 as observed in the same elution fraction from SDS-PAGE analysis (Figs. 3B, 4A), indicating the complex formation of MBP and PS2Aa1 even after being cleaved by proteinase K. Our findings could be explained by MBP's intrinsic chaperone activity, which promotes the proper folding of its fusion partner [24]. MBP is also thought to bind to hydrophobic residues present on unfolded proteins, promoting correct protein folding and thereby increasing the solubility of MBP-tagged proteins [23]. In addition, MBP was previously found to be resistant to thermolysin digestion, which may protect its partner protein from degradation [30].

In this study, we also expressed the full-length PS2Aa1 fused with the 6 × His tag at the N-terminus, so-called His_6-fPS2, using the previously

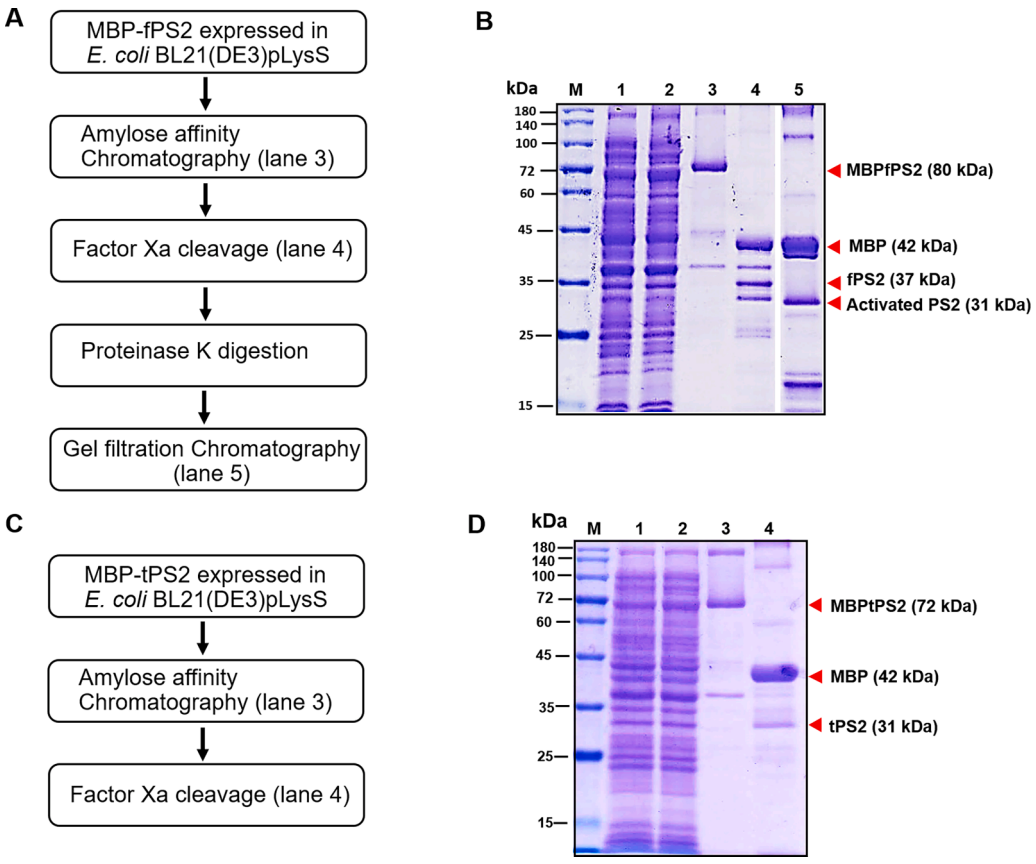

Fig. 3. Purification of PS2Aa1 from soluble MBP-fPS2 and MBP-tPS2 expressed in *E. coli* BL21(DE3)pLysS. Flowcharts of the purification of MBP-fPS2 (A) and MBP-tPS2 (C) fusion proteins. The protein fractions were subjected to SDS-PAGE analysis for MBP-fPS2 (B) and MBP-tPS2 (D). M, molecular weight markers; lane 1, total cell protein before IPTG induction as a negative control; lane 2, total cell protein after IPTG induction; lane 3, the MBP-fPS2 (80 kDa) (B) or MBPtPS2 (72 kDa) (D) fusion protein purified by amylose affinity chromatography; lane 4, the MBP tag cleavage with Factor Xa producing the MBP tag (42 kDa), fPS2 (37 kDa), and tPS2 (31 kDa); lane 5, the final proteinase K-activated PS2Aa1 of MBP-fPS2 fusion protein after gel filtration chromatography (31 kDa) (B). The arrows indicate the molecular masses of the expected protein bands.

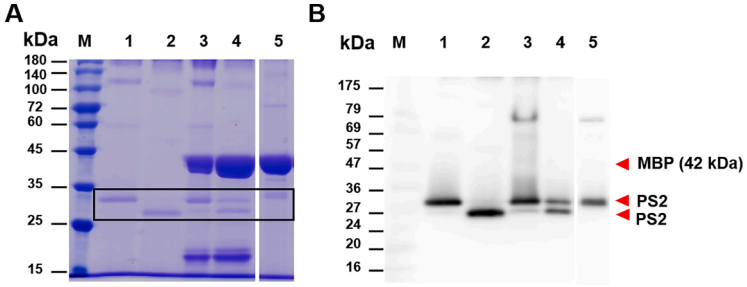

Fig. 4. Analysis of purified recombinant PS2Aa1 from different fusion proteins. SDS-PAGE (A) and western blot analysis of purified recombinant PS2Aa1 using PS2Aa1 polyclonal antibody (B). M, molecular weight makers; the proteinase K-activated His_6-fPS2 after gel filtration chromatography (lanes 1–2); the proteinase K-activated MBP-fPS2 after gel filtration chromatography (lanes 3–4); the purified MBP-tPS2 by amylose affinity chromatography (lane 5). The PS2Aa1 fragments are presented in the box. The arrows indicate the expected protein bands.

described protocols [19]. Unlike the MBP-PS2 fusion proteins, the recombinant His_6-fPS2 accumulated in inclusion bodies (Supplementary Fig. S2), even when the induction temperature was lowered to 18 °C, thereby requiring further solubilization in an alkaline carbonate buffer with a pH of 10.5. The solubilized His_6-fPS2 was purified by Ni-NTA affinity chromatography, followed by proteinase K digestion. Proteinase-K-activated His_6-fPS2 was subjected to gel filtration chromatography to eliminate proteinase-K and other impurities (Fig. 4). This purified His_6-fPS2 protein after protein K activation was subsequently used to compare its cytotoxicity to that of the MBP-PS2 fusion proteins.

Endotoxins, which are immunogenic and highly toxic to humans, can be co-purified with recombinant proteins produced by most *E. coli* hosts, which hinders their application in clinical and biological research [31, 32]. Thus, the endotoxin threshold for clinical applications involving recombinant proteins derived from *E. coli* is established at a value below 1 EU/μg [33]. Here, after endotoxin removal using Triton X-114, the endotoxin levels measured by the Limulus amebocyte lysate (LAL) endotoxin assay of the purified proteins were 0.33, 0.42, and 0.76 EU/μg for MBP-fPS2, MBP-tPS2, and His_6-fPS2, respectively, which are lower than the maximum allowed for biological products (< 1 EU/μg).

3.2. MBP-PS2 fusion proteins exhibited cytotoxicity against human leukemic T cells

After purification, the cytotoxic effects of MBP-fPS2 and MBP-tPS2 fusion proteins against human cancer cells were evaluated using MTT assays with leukemic cancer cell lines (Jurkat and MOLT-4) in comparison with human fibroblast normal cells (Hs68). For MBP-fPS2, both protoxin (non-proteinase K-activated) and proteinase K-activated forms were examined for their cytotoxicity against the tested human cancer cells (Fig. 5A–C). The MBP-fPS2 exhibited no cytotoxicity against Jurkat or MOLT-4 cell lines without proteinase K activation (Fig. 5D, 5E). However, when treated with proteinase K, the cytotoxicity towards MOLT-4 cancer cells increased in a dose-dependent manner (Fig. 5C), with an IC_{50} value of 0.15 μg/mL (Table 1). Jurkat cells were less sensitive to proteinase K-treated MBP-fPS2 than MOLT-4 cells (Fig. 5B), with an IC_{50} value of 0.44 μg/mL (Table 1).

On the other hand, MBP-tPS2 directly exerted cytotoxicity against Jurkat and MOLT-4 cancer cells without proteinase K activation (Fig. 5), with IC_{50} values of approximately 0.03 μg/mL (Table 1). The cytotoxicity of MBP-tPS2 against cancer cells, particularly Jurkat cells, was also found to be superior to that of the proteinase K-activated MBP-fPS2, indicating that the N-terminal processing of PS2Aa1 by cleaving off the first 51 amino acids was critical for the cytotoxicity, at least against the tested leukemic cell lines. It has been demonstrated that the C-terminal processing of PS2Aa1 was not essential for PS2Aa1 cytotoxicity but could induce rapid plasma membrane damage to the cancer cells [10]. Parasporins, like other Bt crystal proteins, require proteolytic processing to exert their cytotoxicity against cancer cells [7]. In particular, the removal of their N-terminal regions is necessary for cytotoxicity. It has been demonstrated that proteolytic cleavage of the N-terminal region of parasporin-1 (81 kDa) resulted in the production of an active form consisting of 15 and 56 kDa polypeptides, rendering it toxic to cancer cells [34]. Parasporin-3, also known as Cry41Aa, has been shown to exhibit cytocidal activity against HL-60 (Human promyelocytic leukemia cells) and HepG2 (Human liver cancer cells) cell lines following proteolytic cleavage. In addition to the importance of the N-terminal region in protein expression, it has been shown that the Cry41Aa toxin's action depends on the N-terminal cleavage at amino acid 40. Deleting the first 40 amino acids from the N-terminus of Cry41Aa has been hypothesized as a potential mechanism for exposing the toxin's receptor-binding site, which results in receptor binding and cancer cell cytotoxicity [35]. Domain I at the N-terminus of PS2Aa1 possesses a high degree of structural diversity, implying that it may be involved in receptor recognition [9]. By removing the N-terminal segment, the receptor-binding site of domain I may be exposed. Additionally, it has been hypothesized that the inhibitory peptide, located immediately upstream of the N-terminal cleavage site of PS2Aa1, interacts with pore-forming domain 2. The removal of this peptide would, therefore, facilitate the domain-2 transition, which is required for pore formation [36].

Table 1
IC_{50} values with 95 % confidence intervals (parentheses) for MBP-tPS2, MBP-fPS2, and His_6-fPS2 with or without proteinase K activation (+ ProK or – ProK) against human leukemic T cells.

Cell line	IC_{50} μg/mL			
	MBP-tPS2 (-ProK)	MBP-fPS2 (-ProK)	MBP-fPS2 (+ProK)	His_6-fPS2 (+ProK)
Jurkat	0.03 (0.02–0.06)	> 0.5	0.44 (0.18–0.74)	0.02 (0.01–0.04)
MOLT-4	0.03 (0.01–0.12)	> 0.5	0.15 (0.07–0.33)	0.03 (0.02–0.07)

In this study, cytotoxic effects of the proteinase K-treated His_6-fPS2 (expressed as inclusion bodies) were also tested for comparison. Results revealed no significant difference in cytotoxicity between MBP-tPS2 and proteinase K-treated His_6-fPS2 samples regardless of being expressed as an insoluble or soluble protein (Fig. 5B, C, and Table 1). In addition, none of the recombinant PS2Aa1 proteins exhibited cytotoxicity against the fibroblast cells, supporting the high selectivity of PS2Aa1 in an active form against the cancer cells (Fig. 5A). Even though MBP-PS2

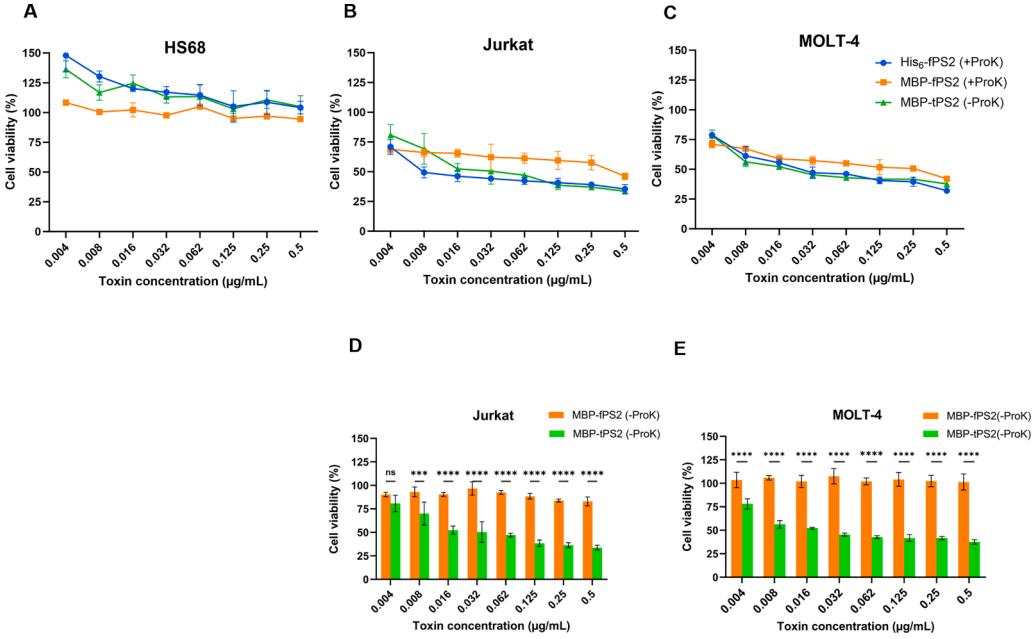

Fig. 5. Cell viability (%) of Hs68 (A) Jurkat (B) and MOLT-4 (C) cells after being treated with His_6-fPS2, MBP-fPS2, and MBP-tPS2 at different concentrations. The proteinase K-treated and non-proteinase K-treated samples are denoted as + ProK and – ProK, respectively. Cell viability (%) of Jurkat (D) and MOLT-4 (E) in response to non-proteinase K-treated MBP-fPS2 and MBP-tPS2 treatments at different concentrations. After 24 h of incubation with various concentrations of protein samples, the percentage of cell viability was determined by MTT assay by comparing the absorbance of each sample to that of the negative control (PBS, pH 7.4). All data are presented as mean ± SD from the triplicate analyses. Statistical significance was analyzed using two-way ANOVA and annotated as follows: **** $p < 0.0001$, *** $p < 0.001$, ns (no significance) $p > 0.9$.

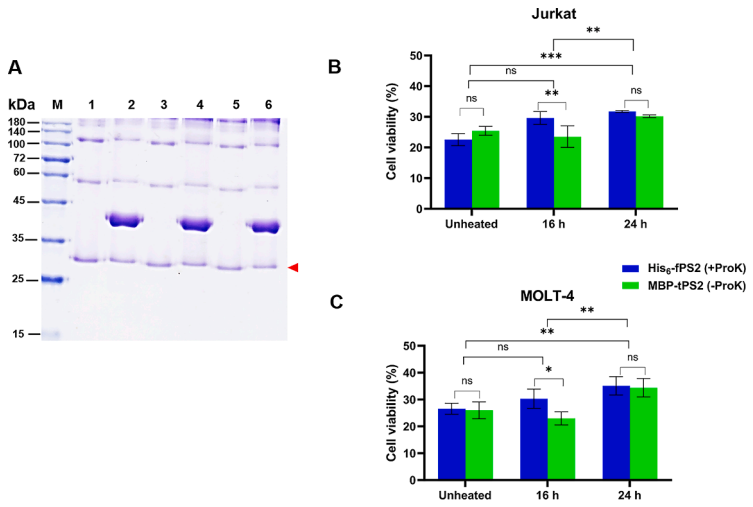

Fig. 6. Functional stability analysis of MBP-tPS2 fusion protein compared with proteinase K-activated His_6-fPS2 after incubation at 37 °C for different time points. (A) SDS-PAGE analysis of purified recombinant MBP-tPS2 and proteinase K-activated His_6-fPS2 proteins upon incubation at 37 °C for 16 and 24 h. M, molecular weight makers; the unheated proteinase K-activated His_6-fPS2 (lane 1) and heated proteinase K-activated His_6-fPS2 for 16 and 24 h (lanes 3 and 5, respectively); the unheated MBP-tPS2 (lane 2) and heated MBP-tPS2 for 16 and 24 h (lanes 4 and 6, respectively). Cell viability (%) of Jurkat (B) and MOLT-4 (C) cells after being treated with 0.5 μg/mL of either unheated or heated proteinase K-activated His_6-PS2 and MBP-tPS2 at 37 °C for 16 and 24 h. All data are presented as mean ± SD from three independent experiments (three replicas each). The arrow indicates the molecular masses of the protein bands at 30–31 kDa used for quantification by gel electrophoresis image analysis software. Statistical significance was analyzed using two-way ANOVA and annotated as follows: ns (no significance) $p > 0.9$, * $p < 0.1$, ** $p < 0.01$, *** $p < 0.001$.

fusion proteins did not lead to any appreciable enhancement of cytotoxicity against tested cancer cells compared with that of the His_6-fPS2, MBP effectively served as a chaperone to protect the PS2Aa1 to form an insoluble aggregated protein.

Because many MBP fusion proteins lose their stability when cleaved from MBP, studies aimed at characterizing the properties and functions of the fusion partners are usually undertaken in the presence of MBP. Furthermore, MBP is a stable monomeric protein with well-defined properties. Therefore, it is unlikely to interfere with fusion protein functional characterization [37]. Because PS2Aa1 could not be entirely separated from MBP during purification in this study, only MBP was employed in a cytotoxic effect assessment to examine its impact on cytotoxicity. MBP alone had no cytotoxicity against any of the tested cell lines, corroborated by the lack of cytotoxicity of non-activated MBP-fPS2 against any of the tested cell lines (Supplementary Figure S3). These data indicate that the observed cytotoxicity against cancer cell lines was primarily due to the activated form of PS2Aa1.

3.3. Functional stability of MBP-tPS2 fusion protein upon incubation at 37°C

According to our previous observations, MBP promotes the solubility of the PS2Aa1 fusion partner through a chaperone-like effect. In addition, MBP and PS2Aa1, whether in full-length or truncated form, remain associated after Factor Xa cleavage. This association complex may contribute to the stability of PS2Aa1. To determine the functional stability of MBP-tPS2 in comparison to proteinase K-activated His_6-fPS2, anti-proliferative activity against MOLT-4 and Jurkat cells was measured after incubation at 37 °C at different time points, comparing with their corresponding un-incubated proteins. Gel electrophoresis image analysis software was used to quantify PS2Aa1 active fragments (30–31 kDa) to 0.5 μg/mL for each sample prior to cell line treatment (Fig. 6A). As demonstrated in Fig. 6B, C, proteinase K-activated His_6-fPS2 incubated at 37 °C for up to 16 h did not impair cytotoxicity towards MOLT-4 and Jurkat cell lines, as evidenced by comparable cytotoxic effects on those two cell lines between incubated and unincubated proteins.

MBP-tPS2, like proteinase K-activated His_6-fPS2, remained cytotoxic to MOLT-4 and Jurkat cell lines when incubated at 37 °C for up to 16 h, inhibiting about 70–80 % of cell proliferation (Fig. 6B, 6C). After 24 h of incubation at 37 °C, MBP-tPS2 and proteinase K-activated His_6-fPS2 exhibited a cytotoxicity reduction of less than 10 % against the MOLT-4 and Jurkat cell lines in comparison to the unincubated proteins (Fig. 6B, 6C). The protein bands associated with the PS2Aa1 active core fragment size were detected in both protein samples after 24 h exposure to 37 °C (Fig. 6A), indicating that the proteins remained undegraded despite the possibility of a modest change in their native conformations. This observation is also consistent with a previous *in silico* prediction based on the prevalence of aliphatic side chains of amino acids, specifically, alanine, valine, leucine, and isoleucine, that PS2 is relatively thermostable, with an Aliphatic index of 62.54- 75.00 [38]. Overall, the results show that MBP-tPS2 and proteinase K-activated His_6-fPS2 remained active throughout a 24 h incubation at 37 °C.

4. Conclusions

In conclusion, this is the first report that successfully expressed and purified soluble PS2Aa1 fused with the MBP tag in *E. coli*. The chaperone-like ability of MBP confers several benefits to the PS2Aa1 fusion partner by improving the solubility, folding, and stability of the PS2Aa1 protein. The enhanced solubility of MBP-tPS2 renders it an appropriate platform for functional analysis and therapeutic applications. For example, an MBP-based pull-down test using the MBP-tPS2 fusion protein as the bait protein can be utilized to identify the putative binding protein(s) to uncover the mechanism of cancer cell selectivity. The current strategy and production system also hold considerable potential for efficient and cost-effective large-scale PS2Aa1 manufacturing for future therapeutic applications.

Funding

This research was funded by Mahidol University (Fundamental Fund: fiscal year 2023 by National Science Research and Innovation Fund (NSRF)), the National Research Council of Thailand (NRCT), and Mahidol University (grant number NRCT5-RSA63015–06) to P.B.

CRediT authorship contribution statement

Monrudee Srisaisap: Writing – review & editing, Validation, Methodology, Investigation, Formal analysis. **Thanya Suwankhajit:** Writing – review & editing, Methodology, Investigation, Formal analysis. **Panadda Boonserm:** Writing – review & editing, Writing – original draft, Visualization, Validation, Supervision, Project administration, Methodology, Investigation, Funding acquisition, Formal analysis, Conceptualization.

Declaration of competing interest

The authors declare that they have no known competing financial interests or personal relationships that could have appeared to influence the work reported in this paper.

Data availability

Data will be made available on request.

Acknowledgments

The authors gratefully acknowledge the Institute of Molecular Biosciences, Mahidol University, Thailand, for the facilities. The authors are also thankful to Panat Anuracpreeda and his team for their assistance in producing rabbit polyclonal antibodies and Thanapon Kunlawatwimon, Tharathip Hemthanon, Pongsatorn Khunrach, and Pasin Jammor for their assistance in analyzing the data.

Supplementary materials

Supplementary material associated with this article can be found, in the online version, at doi:10.1016/j.btre.2024.e00851.

References

[1] L. Palma, D. Muñoz, C. Berry, J. Murillo, P. Caballero, *Bacillus thuringiensis* toxins: an overview of their biocidal activity, Toxins 6 (2014) 3296–3325 (Basel).
[2] D. Valtierra-de-Luis, M. Villanueva, C. Berry, P. Caballero, Potential for *Bacillus thuringiensis* and other bacterial toxins as biological control agents to combat dipteran pests of medical and agronomic importance, Toxins 12 (2020) (Basel).
[3] A. Bravo, S.S. Gill, M. Soberon, Mode of action of *Bacillus thuringiensis* Cry and Cyt toxins and their potential for insect control, Toxicon 49 (2007) 423–435.
[4] E. Mizuki, M. Ohba, T. Akao, S. Yamashita, H. Saitoh, Y.J.J.O.A.M. Park, Unique activity associated with non-insecticidal *Bacillus thuringiensis* parasporal inclusions: *in vitro* cell-killing action on human cancer cells, J. Appl. Microbiol. 86 (1999) 477–486.
[5] E. Mizuki, Y.S. Park, H. Saitoh, S. Yamashita, T. Akao, K. Higuchi, M. Ohba, Parasporin, a human leukemic cell-recognizing parasporal protein of *Bacillus thuringiensis*, Clin. Diagn. Lab. Immunol. 7 (2000) 625–634.
[6] N. Crickmore, C. Berry, S. Panneerselvam, R. Mishra, T.R. Connor, B.C.J. Bonning, A structure-based nomenclature for *Bacillus thuringiensis* and other bacteria-derived pesticidal proteins, J. Invertebr. Pathol. 186 (2021) 107438.
[7] M. Ohba, E. Mizuki, A. Uemori, Parasporin, a new anticancer protein group from *Bacillus thuringiensis*, Anticancer Res. 29 (2009) 427–433.
[8] C. Xu, B.C. Wang, Z. Yu, M. Sun, Structural insights into *Bacillus thuringiens*is Cry, Cyt and parasporin toxins, Toxins 6 (2014) 2732–2770 (Basel).
[9] T. Akiba, Y. Abe, S. Kitada, Y. Kusaka, A. Ito, T. Ichimatsu, H. Katayama, T. Akao, K. Higuchi, E. Mizuki, M. Ohba, R. Kanai, K. Harata, Crystal structure of the parasporin-2 *Bacillus thuringiensis* toxin that recognizes cancer cells, J. Mol. Biol. 386 (2009) 121–133.
[10] S. Kitada, Y. Abe, H. Shimada, Y. Kusaka, Y. Matsuo, H. Katayama, S. Okumura, T. Akao, E. Mizuki, O. Kuge, Y. Sasaguri, M. Ohba, A. Ito, Cytocidal actions of parasporin-2, an anti-tumor crystal toxin from *Bacillus thuringiensis*, JBC 281 (2006) 26350–26360.
[11] T. Hayakawa, R. Kanagawa, Y. Kotani, M. Kimura, M. Yamagiwa, Y. Yamane, S. Takebe, H. Sakai, Parasporin-2Ab, a newly isolated cytotoxic crystal protein from *Bacillus thuringiensis*, Curr. Microbiol. 55 (2007) 278–283.
[12] A. Ito, Y. Sasaguri, S. Kitada, Y. Kusaka, K. Kuwano, K. Masutomi, E. Mizuki, T. Akao, M. Ohba, A *Bacillus thuringiensis* crystal protein with selective cytocidal action to human cells, JBC 279 (2004) 21282–21286.
[13] S. Kitada, Y. Abe, T. Maeda, H. Shimada, Parasporin-2 requires GPI-anchored proteins for the efficient cytocidal action to human hepatoma cells, Toxicology 264 (2009) 80–88.
[14] Y. Abe, H. Inoue, H. Ashida, Y. Maeda, T. Kinoshita, S. Kitada, Glycan region of GPI anchored-protein is required for cytocidal oligomerization of an anticancer parasporin-2, Cry46Aa1 protein, from *Bacillus thuringiensis* strain A1547, J. Invertebr. Pathol. 142 (2017) 71–81.
[15] A. Periyasamy, P. Kkani, B. Chandrasekaran, S. Ponnusamy, S. Viswanathan, P. Selvanayagam, S. Rajaiah, Screening and characterization of a non-insecticidal *Bacillus thuringiensis* strain producing parasporal protein with selective toxicity against human colon cancer cell lines, Ann. Microbiol. 66 (2016) 1167–1178.
[16] M.O. Suárez-Barrera, L. Visser, E.H. Pinzón-Reyes, P. Rondón Villarreal, J. S. Alarcón-Aldana, N.J. Rueda-Forero, Site-directed mutants of parasporin ps2aa1 with enhanced cytotoxic activity in colorectal cancer cell lines, Molecules 27 (2022).
[17] K. Brasseur, P. Auger, E. Asselin, S. Parent, J.C. Cote, M. Sirois, Parasporin-2 from a new Bacillus thuringiensis 4R2 strain induces caspases activation and apoptosis in human cancer cells, PLoS One 10 (2015) e0135106.
[18] S. Kanwal, P. Boonserm, Study on cellular localization of Bin toxin and its apoptosis-inducing effect on human nasopharyngeal carcinoma cells, Curr.Cancer Drug Targets 23 (2023) 388–399.
[19] W. Chankamngoen, T. Janvilisri, B. Promdonkoy, P. Boonserm, *In vitro* analysis of the anticancer activity of *Lysinibacillus sphaericus* binary toxin in human cancer cell lines, 3, Biotech 10 (2020) 365.
[20] D.S. Waugh, Making the most of affinity tags, Trends Biotechnol. 23 (2005) 316–320.
[21] P. Sun, J.E. Tropea, D.S. Waugh, Enhancing the solubility of recombinant proteins in *Escherichia coli* by using hexahistidine-tagged maltose-binding protein as a fusion partner, Methods Mol. Biol. 705 (2011) 259–274 (Clifton, N.J.
[22] G.T. Lountos, J.E. Tropea, D. Zhang, A.G. Jobson, Y. Pommier, R.H. Shoemaker, D. S. Waugh, Crystal structure of checkpoint kinase 2 in complex with NSC 109555, a potent and selective inhibitor, Protein Sci. 18 (2009) 92–100.
[23] R.B. Kapust, D.S. Waugh, *Escherichia coli* maltose-binding protein is uncommonly effective at promoting the solubility of polypeptides to which it is fused, Protein Sci. 8 (1999) 1668–1674.
[24] H. Bach, Y. Mazor, S. Shaky, A. Shoham-Lev, Y. Berdichevsky, D.L. Gutnick, I. Benhar, *Escherichia coli* maltose-binding protein as a molecular chaperone for recombinant intracellular cytoplasmic single-chain antibodies, J. Mol. Biol. 312 (2001) 79–93.
[25] S. Raran-Kurussi, D.S. Waugh, The ability to enhance the solubility of its fusion partners is an intrinsic property of maltose-binding protein but their folding is either spontaneous or chaperone-mediated, PLoS One 7 (2012) e49589.
[26] P. Anuracpreeda, C. Wanichanon, R. Chawengkirtikul, K. Chaithirayanon, P. Sobhon, *Fasciola gigantica*: immunodiagnosis of fasciolosis by detection of circulating 28.5 kDa tegumental antigen, Exp. Parasitol. 123 (2009) 334–340.
[27] S. Costa, A. Almeida, A. Castro, L. Domingues, Fusion tags for protein solubility, purification and immunogenicity in *Escherichia coli*: the novel Fh8 system, Front. Microbiol. 5 (2014) 63.
[28] S. Nallamsetty, D.S. Waugh, Mutations that alter the equilibrium between open and closed conformations of Escherichia coli maltose-binding protein impede its ability to enhance the solubility of passenger proteins, BBRC 364 (2007) 639–644.
[29] R. Wang, X. Gu, Z. Zhuang, Y. Zhong, H. Yang, S. Wang, Screening and molecular evolution of a single chain variable fragment antibody (scfv) against Citreoviridin toxin, J. Agric. Food Chem. 64 (2016) 7640–7648.
[30] C. Park, S. Zhou, J. Gilmore, S. Marqusee, Energetics-based protein profiling on a proteomic scale: identification of proteins resistant to proteolysis, J. Mol. Biol. 368 (2007) 1426–1437.
[31] Q. Liu, Y. Li, X. Zhao, X. Yang, Q. Liu, Q. Kong, Construction of *Escherichia coli* mutant with decreased endotoxic activity by modifying lipid A structure, Mar. Drugs 13 (2015) 3388–3406.
[32] P.O. Magalhães, A.M. Lopes, P.G. Mazzola, C. Rangel-Yagui, T.C. Penna, A. Pessoa, Methods of endotoxin removal from biological preparations: a review, JPPS 10 (2007) 388–404.
[33] H. Schwarz, M. Schmittner, A. Duschl, J. Horejs-Hoeck, Residual endotoxin contaminations in recombinant proteins are sufficient to activate human CD1c+ dendritic cells, PLoS One 9 (2014) e113840.
[34] H. Katayama, Y. Kusaka, H. Yokota, T. Akao, M. Kojima, O. Nakamura, E. Mekada, E. Mizuki, Parasporin-1, a novel cytotoxic protein from *Bacillus thuringiensis*, induces Ca^{2+} influx and a sustained elevation of the cytoplasmic Ca^{2+} concentration in toxin-sensitive cells, J. Biol. Chem. 282 (2007) 7742–7752.
[35] W. Souissi, A. Kaloki, S. Etherington, B. Domanska, M.J. West, N. Crickmore, Differential proteolytic activation of the *Bacillus thuringiensis* Cry41Aa parasporin modulates its anticancer effect, J. Biochem. 476 (2019) 3805–3816.
[36] T. Akiba, S. Okumura, Parasporins 1 and 2: their structure and activity, J. Invertebr. Pathol. 142 (2017) 44–49.
[37] A.A. Momin, U.F.S. Hameed, S.T. Arold, Passenger sequences can promote interlaced dimers in a common variant of the maltose-binding protein, Sci.Rep 9 (2019) 20396.
[38] N. Aktar, M. Karim, S. Khan, M. Rahman, A. Begum, M. Hoq, In silico studies of parasporin proteins: structural and functional insights and proposed cancer cell killing mechanism for parasporin 5 and 6, Microb. Bioact. 2 (1) (2019).